European Journal of Technique

journal homepage: https://dergipark.org.tr/en/pub/ejt

Vol.14, No.1, 2024

Research Article

Design and Performance Analysis of Single-Phase Squirrel-Cage Induction Machine with High Efficiency

Serhat Akşun[1*], Sezai Taşkın[2], Ali Bakbak[3]

[1] Volt Elektrik Motor Company, Kazım Karabekir Cad. No:84 Kemalpaşa-Izmir, Türkiye (e-mail: serhat.aksun@voltmotor.com.tr).
[2*3] Manisa Celal Bayar University, Electrical and Electronics Engineering Department, 45140, Yunusemre, Manisa, Türkiye.
(e-mail: sezai.taskin@cbu.edu.tr), (ali.bakbak@cbu.edu.tr)

ARTICLE INFO

Received: March, 09, 2024
Revised: May., 15. 2024
Accepted: May, 15. 2024

Keywords:
Electrical machine design
Single phase induction motor
IE2 Efficiency
IEC 60034-2-1:2014

Corresponding author: *Sezai Taşkın*

ISSN: *2536-5010* | e-ISSN: *2536-5134*

DOI: https://doi.org/10.36222/ejt.1449620

ABSTRACT

This study presents an approach to designing single-phase squirrel-cage induction motors with a focus on achieving high efficiency. The objective is to improve the performance of the motors, particularly in meeting IE2 efficiency standards, without compromising on power or reliability. Specifically addressed is a single-phase squirrel-cage induction motor with a rated power of 0.55 kW. Through comprehensive design iterations involving dimensioning, slot-pole selection, and parametric optimization of stator and rotor geometry, the efficiency of the single-phase squirrel-cage induction motor has been improved from the current market design of 64.9% to a minimum of 77.1%, as defined in the IEC 60034-30 standard. Analysis includes key parameters such as slot opening, end-ring length, and rotor bar width, highlighting their significant influence on performance metrics. Experimental validation, conducted at an ISO/EN 17025 accredited R&D Laboratory, confirms the design improvements, achieving an efficiency of 80.1%. This research highlights the potential for significant energy savings across various applications by improving the efficiency of single-phase squirrel-cage induction motors to meet IE2 standards.

1. INTRODUCTION

The development of energy-efficient electric motors has great significance to address sustainability and energy conservation challenges. Most small power, generally below 2 kW, induction machines are operated with single-phase power supplies [1]. SPIMs are extensively used in appliances, small machinery, and domestic applications, such as compressors, air conditioners, heating-circulating pumps, fans, centrifugal pumps, vacuum cleaners, sewing, washing and milking machines, and so on [1]. Due to their wide range of applications, achieving high efficiency in SPIMs is high importance [2,3]. According to new energy efficiency regulations (EU) 2019/1781 and amending (EU)2021/341 starting 1st July 2023, the SPIMs must provide IE2 efficiency level in Europe [4]. Efficiency standards and regulations play a crucial role in driving the development of energy-efficient induction motors. The International Electrotechnical Commission (IEC) has established standards, including IE2 efficiency requirements, to encourage the adoption of motors with higher efficiency ratings. Compliance with these standards ensures that motors meet specific efficiency requirements, contributing to energy savings and reduced environmental impact.

In recent years, various research endeavors have focused on improving the performance of SPIM motors, with extensive analysis undertaken on aspects encompassing motor modeling, design, manufacturing, and control. Researchers have initially prioritized the development of more accurate models to assess SPIM losses, factoring in phenomena such as eddy currents and nonlinear effects such as magnetic saturation affecting motor components [5].

The focus of many research efforts has been on optimizing the configuration of the squirrel-cage rotor in electric motors. The geometry and layout of the rotor bars play a critical role in determining the motor's efficiency, power factor, and starting torque [6]. Various designs for rotor slots, including trapezoidal, oval, circular, rectangular, and pentagonal shapes, as well as different configurations of rotor bars such as open, semi-closed, and closed, with varying depths, have been thoroughly investigated [7]. Additionally, studies have examined the impact of factors such as the size of the rotor bar slot opening and the aspect ratio of the bar's width to its height. Despite advancements in rotor design methodologies, the process still heavily relies on the experience and intuition of the designer. Incorporating optimization algorithms and other artificial techniques into the design process has become increasingly necessary. The selection of the number of rotor bars, in conjunction with the combination of pole pairs and

stator slots, significantly influences the motor's efficiency. Furthermore, experimental materials have been utilized in the construction of parts for SPIMs, with aluminum rotors being replaced by die-cast copper ones. Among various manufacturing processes, die-casting has emerged as the most efficient method for mass-producing squirrel-cage components in SPIMs [8].

The characteristics of capacitors represent another significant factor. Researches have centered on several key areas such as determining the most suitable placement of the capacitor, selecting the optimal value of the capacitor, examining its influence on the phase shift between primary and auxiliary winding currents, and evaluating how this phase shift affects the quality of the motor's torque. Increasing capacitance boosts starting torque, although at the expense of motor efficiency beyond a certain point. Consequently, determining the ideal value for the run capacitor is important.

Factors such as poor power factor, low starting torque, and unbalanced magnetic fields pose challenges in achieving high efficiency. Enhanced winding designs, such as the split-phase, capacitor start, and capacitor run configurations, have been investigated to optimize performance. These designs help mitigate power factor issues and increase motor efficiency by improving the distribution of magnetic fields [9]. Power factor correction methods have also been explored to enhance the efficiency of SPIMs. Techniques such as capacitor banks, reactive power compensation, and active power factor correction circuits have been employed to improve power factor and reduce energy losses [10].

In the manufacturing process, the optimal design for SPIM is presented in [11], aiming to obtain the dimensions and electrical parameters of a SPIM. In addition, [12] delves into a study focusing on a single-phase permanent slip capacitor induction motor for a washing machine with the parameters of 373 W, 4 pole, 220 V, 50 Hz.

This study represents a significant contribution to the field of single-phase squirrel-cage induction motors. By focusing on the design, analysis, and performance testing of a 0.55 kW 4P SPIM with high efficiency (IE2), our research fills a crucial gap in current knowledge and industry practice. Utilizing Siemens Simcenter SPEED software for motor design, notable improvements in efficiency have been achieved, enhancing the SPIM's performance from the current market standard of 64.9% to a minimum of 77.1%, as defined in the IEC 60034-30 standard. This advancement not only aligns with global energy efficiency regulations but also offers tangible benefits to industries and households worldwide. A comprehensive layout of the design process, test methods, and systems is provided in this paper, offering valuable insights for researchers, engineers, and practitioners in the field. Meticulous attention to detail in each section, from design steps to prototyping and performance testing, aims to set a new standard for SPIM efficiency and contribute to the ongoing evolution of sustainable motor technologies.

2. ELECTROMAGNETIC DESIGN

A SPIM can be classified into different types based on its starting mechanism, namely (i) split phase, (ii) capacitor start, (iii) shaded pole, and (iv) repulsion type [13]. This study focuses on examining the characteristics of capacitor start motors. The single-phase capacitor start induction motor is classified into three specific types as follows.

(i) Two-value capacitor motor
(ii) Permanent-split capacitor motor
(iii) Capacitor-start induction run motor

In this study, a permanent-split capacitor motor is considered. The design algorithm of the motor is given in Figure 1. The operations in each step of the algorithm have been explained in detail in the following sections. Performance calculations, including electromagnetic analysis, have been conducted using FEA. The prototype of the designed motor was produced and tested.

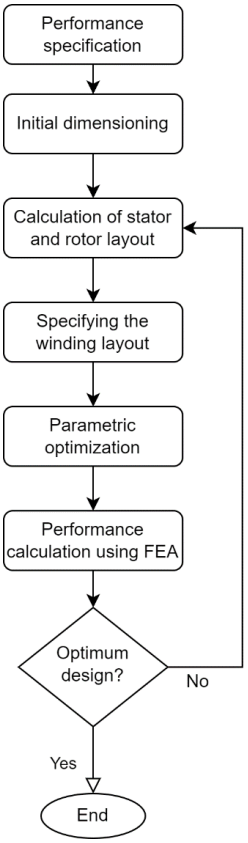

Figure 1. Design algorithm

2.1. Performance specifications

The specified motor is intended for use in milking machines. In the field, most milking machines use motors with the following specifications 550W, 4 poles (4P), 230V, 50Hz. Other requirements for milking machine motors include:

(i) Moderate starting torque: 0.3-0.6 times the nominal torque.
(ii) Low starting current: 4-5 times the nominal current.
(iii) High breakdown torque: 2-3 times the nominal torque.
(iv) Max. Capacitor Voltage: 400V.
(v) Nominal efficiency is 77.1% and minimum efficiency is 73.7% according to IEC 60034-30.

To prevent excessive temperature rise, current densities should be kept below 7 A/mm² for aux winding and 4 A/mm² for main winding. Temperature rise up is maximum 80°C for aux winding and main winding.

The design targets specified in Table I. In the table; *ILr* is the starting current, *In* is the nominal current, *TLr* is the starting torque, *TBr* is the breakdown torque and *Tn* is the nominal torque. The two target values specified for some parameters, such as speed and efficiency, represent a range within which

the parameter value is acceptable. This range accounts for variations that may occur due to different operating conditions or manufacturing tolerances. Therefore, if the parameter value falls within this range, it is considered satisfactory for our design targets.

TABLE I
DESIGN TARGETS

Parameter	Unit	Target value
Power	*W*	550
Speed	*rpm*	1400-1450
Torque	*Nm*	3.66
Voltage	*V*	220
Frequency	*Hz*	50
Efficiency	-	73.7-77.1
ILr/In	-	4-5
TLr/Tn	-	0.3-0.6
TBr/Tn	-	2-3
Capacitor voltage	*V*	<400
Current density of main winding	-	<4
Current density of aux winding	-	<7

2.2. Dimensioning

2.2.1 Stator Outer and Inner diameter

The machine utilization factor (*Cu*) is used to determine the stator's outer diameter and stack length, calculated according to Equation 1.

$$C_u = D_o^2.L \quad (1)$$

where *Do* is the outer diameter, and *L* is the calculated stack length.

Figure 2 shows the utilization factor (*Cu*) specifically for 4-pole (4P) induction machines.

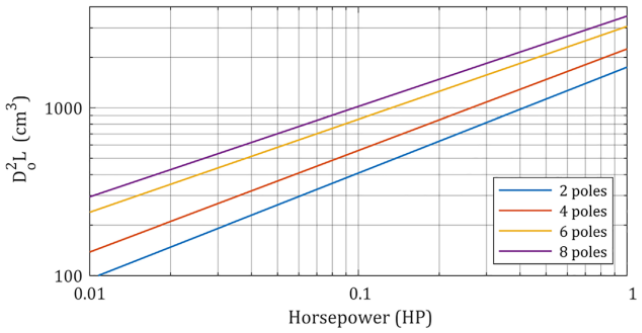

Figure 2. Machine utilization factor [7]

The optimal ratio for the inner diameter to outer diameter (*Di/Do*) is typically specified as given in Table II [1].

TABLE II
STATOR INNER/OUTER DIAMETER RATIO

2P	2	4	6	8
$\frac{D_i}{D_o}$	0.54-0.58	0.61-0.63	0.68-0.71	0.72-0.74

2.2.2 Stator and rotor slot combination

The combination of stator and rotor slot numbers plays a crucial role in motor operation. Determining the right combination is essential to avoid various issues during the motor operation such as electromagnetic noise, parasitic torque in the torque-speed curve and low efficiency.

In the case of 4-pole (4P) motor, a stator slot number of 36 is selected. For this stator slot number, different rotor slot numbers are investigated according to reference [1]. To mitigate magnetic noise and parasitic torque, a rotor slot number of 28 is determined as the optimal configuration. Failing to select the appropriate slot combination may lead to the following issues: electromagnetic noise, synchronous torque problems in the torque-speed curve, and reduced efficiency. To address these concerns, it is recommended to refer to Table III for the stator-rotor slot combination.

TABLE III
STATOR ROTOR SLOT NUMBER COMBINATION

2P	Stator slot number (Ns)	Rotor slot number (Nr)
2	24	18, 20, 22, 28, 30, 33, 34
	36	25, 27, 28, 29, 30, 43
	48	30, 37, 39, 40, 41
4	24	16, 18, 20, 30, 33, 34, 35, 36
	36	**28**, 30, 32, 34, 45, 48
	48	36, 40, 44, 57, 59
	72	42, 48, 54, 56, 60, 61, 62, 68, 76
6	36	20, 22, 28, 44, 47, 49
	54	34, 36, 38, 40, 44, 46
	72	44, 46, 50, 60, 61, 62, 82, 83

2.2.3 Air gap and dimensioning stator and rotor slots

The air gap (*g*) dimension for 4-pole (4P) motor is calculated using Equation 2 [1].

$$g = \left(0{,}1 + 0{,}012.\sqrt[3]{Pn}\right) \quad (2)$$

For the specified motor, the air gap (*g*) is found as 0.2 mm.

The dimensioning of stator slots in the motor design is taken into account with the following important parameters:

(i) Production Capability: The design should consider the practical constraints and capabilities of the production process.

(ii) Magnetic Flux Density of Stator Yoke (at *Hsty*): The magnetic flux density in the stator yoke should be controlled to limit iron losses. A maximum preferred value of 1.6 Tesla (T) is considered.

(iii) Magnetic Flux Density of Stator Tooth Width: The magnetic flux density in the stator tooth width is another crucial factor to optimize for efficient motor performance.

To determine optimum values for stator rotor slots, parametric analysis is used. Optimum values are given in Table IV. The dimensions represented by the parameters in the Table IV are depicted in Figure 3.

TABLE IV
STATOR PARAMETRIC DIMENSION

Parameters	Dimensioning Boundaries (mm)	Optimum value (mm)
Hsty	9-10	9.5
Wstt	3-4	3.38
Hso	0.5-1	0.75
Sso	2-3	2.23
Hrts	14.5-15.5	14.79
Wrtt	4-5	4.79
Rs	0-0.5	0.2
Sro	0.5-1.5	1

The dimensions are carefully determined to attain the best possible motor performance and efficiency. Considering the selected stator and rotor slot combinations, as well as the dimensioning requirements, the lamination design is successfully finalized. The specific design of the lamination is given in Figure 3.

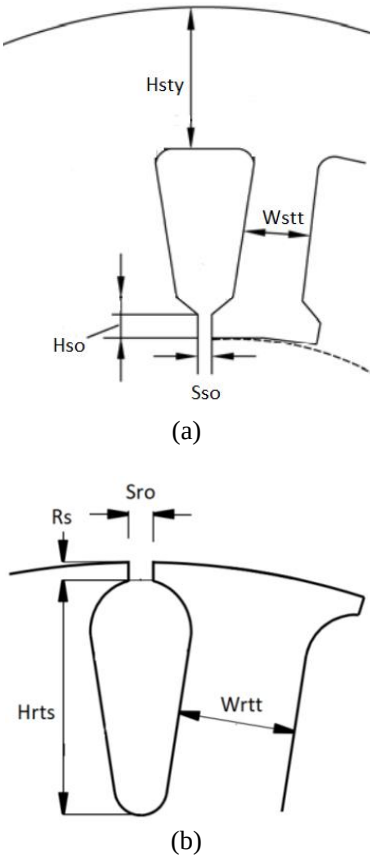

Figure 3. Slot parameters of (a) stator and (b) rotor.

In parametric optimization, one of the key parameters is the height of the rotor bars. Although increasing this height also increases the starting torque, it reduces efficiency. Therefore, the *Hrts* value that provides the required starting torque with the highest efficiency has been selected. The impact of the *Hrts* value on efficiency and starting torque is shown in Figure 4.

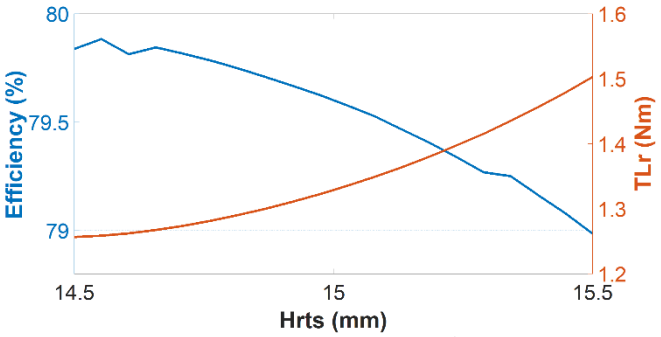

Figure 4. Parametrization of Hrts

These dimensions are established with the aim of ensuring proper casting in the rotor slots, while simultaneously achieving desirable performance outcomes in terms of speed, efficiency, and the torque-speed curve.

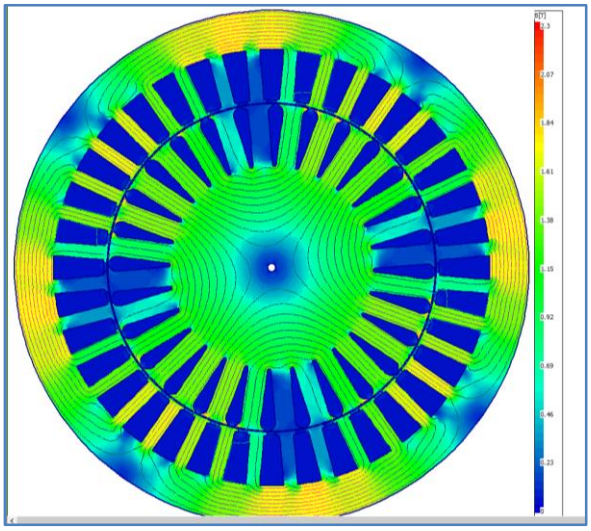

Figure 5. Magnetic flux density distribution of the machine

The Finite Element Method (FEM) analysis yielded magnetic flux density results, which are presented in Figure 5. The analysis indicates that there is no saturation observed in the steel material. Table V presents the magnetic flux density values for specific points."

2.2.4 Winding Design

In the winding design phase, the number of turns per pole, wire diameters, and the winding scheme are determined based on the following criteria:

(i) Number of Turns (*Nm*) Calculation: The number of turns in the main winding is determined based on the electromagnetic force (EMF) using the Equation 3.

$$E_m = \pi.\sqrt{2}.\Phi_m.Nm.K_{wm}.f \quad (3)$$

where K_{wm} represents the winding factor and f is the frequency.

(ii) Wire Diameter Determination: Wire diameters are chosen considering factors such as current densities, copper losses, and slot fill factor. The slot fill factor area should not

exceed 0.45 to ensure manufacturability. The wire diameter is calculated using Equation 4.

$$J = \frac{I}{\frac{\Pi . d^2}{4}} \quad (4)$$

where J represents the current density, I is the current, and d is the wire diameter. Based on the criteria, the following specifications are determined:

- Number of turns in the main winding (*N_m*): 15-18-50-50.
- Number of turns in the auxiliary winding (*N_aux*): 45-49-68 / 45-49.
- Wire diameter of the main winding: 0.8mm
- Wire diameter of the auxiliary winding: 0.7mm

The distributed winding scheme, as depicted in Figure 6, is utilized in the motor design.

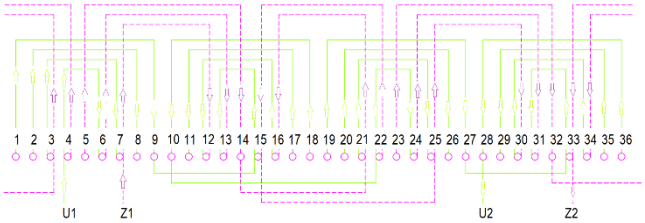

Figure 6. Winding scheme

3. ELECTROMAGNETIC ANALYSIS

The design parameters are given in Table V. The torque-speed curve for the motor design is shown in Figure 7. This curve shows the relationship between the motor's torque output and its rotational speed. By examining the torque-speed curve, important information for the motor performance characteristics can be obtained. As seen in Figure 7, the starting torque is 1.3 Nm, and maximum torque is 6.7 Nm at the 1285 rpm.

The torque-speed curve demonstrates that there is no presence of synchronous torque. This indicates that the determined combination of stator and rotor slot numbers is appropriate.

TABLE V
ANALYSIS RESULTS

Parameter	Unit	Result
Current	*A*	3.2
Speed	*rpm*	1433
Rated torque	*Nm*	3.66
Rated power	*W*	550
Efficiency		78.9
Locked rotor torque p.u		0.4
Locked rotor current p.u		3.8
Breakdown torque p.u		2.14
Capacitor voltage	*V*	330
Stator yoke magnetic flux	*T*	1.59
Stator tooth magnetic flux	*T*	1.53
Rotor tooth magnetic flux	*T*	1.4

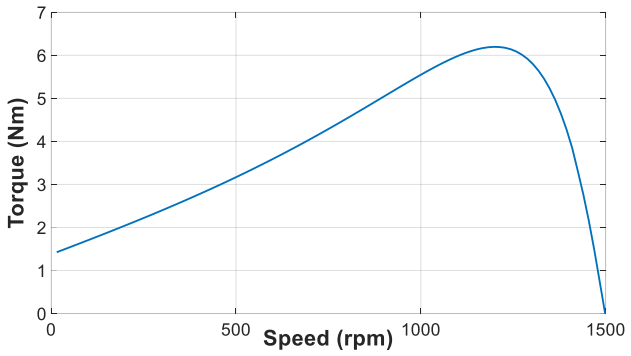

Figure 7. Torque-speed curve

The temporal torque characteristic is given in Figure 8, showing a well-balanced graph with no detectable harmonic effects. The FEM results and analytical analysis both confirm that the design targets have been successfully achieved.

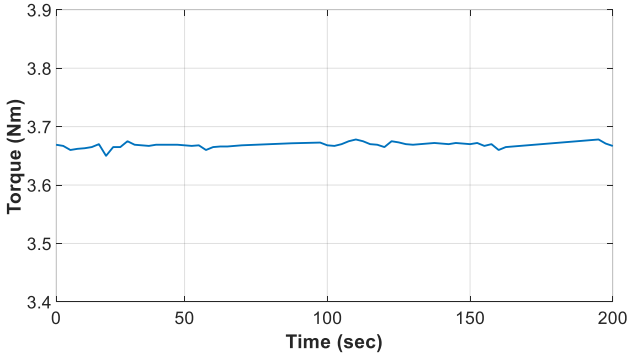

Figure 8. Torque profile over time

4. EXPERIMENTAL RESULTS

During the prototyping phase, it is crucial to ensure that semi-finished products, such as shafts and housings, meet the specified tolerances. Deviations from the required tolerances can result in an unstable air gap. An unstable air gap can lead to increased losses and harmonics, the occurrence of synchronous torque on the torque-speed curve, and the potential for magnetic sound generation. Therefore, meticulous attention should be given to maintaining the desired tolerances to ensure a rigid air gap and mitigate these adverse effects. The prototyped motor is shown in Figure 9.

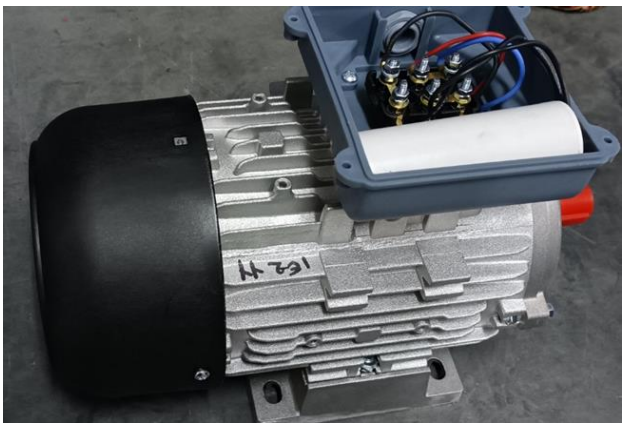

Figure 9. The prototyped motor

For the motor testing process, a torque-controlled dynamometer is used. This dynamometer incorporates a power analyzer, torque sensor, and speed sensor. The power analyzer provides the measurement of current, frequency, voltage, and power factor. The torque and speed sensor allow for the measurement of torque and speed, respectively. Experimental set-up of the system is shown in Figure 10 and 11.

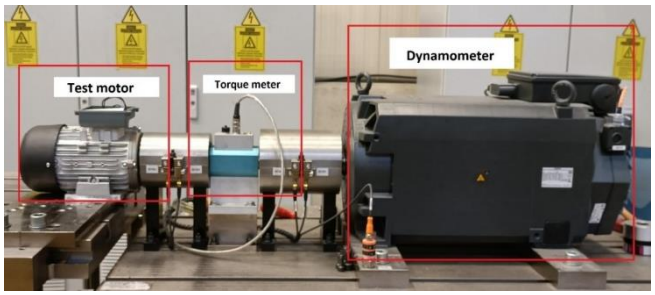

Figure 10. Test system

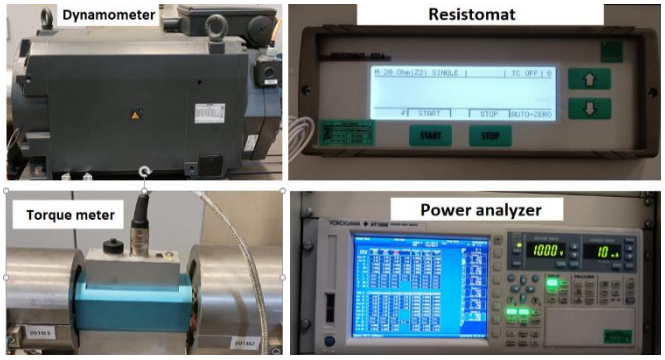

Figure 11. Other components of the test system

By utilizing the values obtained from the power analyzer, electrical power can be calculated, while the values acquired from the torque and speed sensor enable the determination of mechanical power. The combination of electrical and mechanical power facilitates the calculation of motor efficiency. It is essential to ensure proper alignment and coupling between the motor and dynamometer during testing. Aligning them in the same line is crucial to obtain reliable test results and ensure that the measured efficiency corresponds to the nominal value. The test procedure for efficiency measurement is outlined as follows [14]:

(i) Couple the motor to the dynamometer.

(ii) Apply a load to the motor up to its rated power.

(iii) Calculate the efficiency.

To measure locked rotor current, locked rotor torque, and breakdown torque, the following test procedure is specified [10]:

(i) Couple the motor to the dynamometer.

(ii) Initiate the locked rotor condition.

(iii) Measure the torque and current.

Following these testing procedures ensures accurate assessment of motor performance, including efficiency, locked rotor characteristics, and breakdown torque. All the tests are conducted in accordance with the IEC 60034-2-1 standard, which outlines three efficiency determination methods:

Method 2-1-1A: This method is applicable to all single-phase machines.

Method 2-1-1B: This method is used for three-phase machines with a rated output power of up to 2 MW.

Method 2-1-1C: This method is employed for three-phase machines with a rated output power exceeding 2 MW.

In this study, Method 2-1-1A is utilized to determine the efficiency of the motor. According to this method, the motor is loaded to its rated power until thermal equilibrium is achieved, with a rate of change of 1 K or less per half hour. Measurements of voltage, current, electrical power, speed (n), torque (T), and temperatures are saved during the test. The temperature measurement graph for full-load operation starting at 30 degrees Celsius is given in Figure 12. The temperatures reached by the motor in a steady state are within the permitted limits.

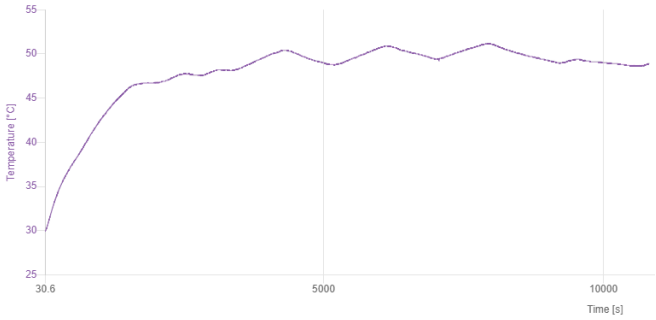

Figure 12. Temperature rise up of the motor

The test results are compared with the analysis results in Table VI. The results show that the design targets are successfully achieved based on the comparison of these results.

TABLE VI
COMPARING OF THE ANALYSIS AND TEST RESULTS

Parameter	Unit	Analysis Result	Test Result
Current	*A*	3.2	3.3
Speed	*rpm*	1433	1440
Rated torque	*Nm*	3.66	3.66
Rated power	*W*	550	550
Efficiency	-	77.8	80.1
Locked rotor torque p.u	-	0.4	0.5
Locked rotor current p.u	-	3.8	3.9
Breakdown torque p.u	-	2.14	2.1
Capacitor voltage	*V*	330	360
Stator yoke magnetic flux	*T*	1.59	Design value
Stator tooth magnetic flux	*T*	1.53	
Stator tooth magnetic flux	*T*	1.4	

5. CONCLUSION

In this study, the development and performance testing of a 0.55 kW single-phase induction motor with high efficiency in accordance with the IE2 class requirements are successfully accomplished. The design process involved proper dimensioning, selection of the slot-pole combination, parametric optimization of the stator and rotor geometry, and

rigorous finite element analyses to validate the design. By analyzing the impact of parameters such as slot opening, end-ring length, and rotor bar width, we identify the specific design enhancements responsible for optimizing the performance of the SPIM. Additionally, the significance of these modifications in aligning the SPIM with IE2 efficiency standards and maximizing energy savings across various industrial and residential applications is discussed.

The analysis results demonstrated that the designed SPIM achieved notable performance specifications, including a power factor of 0.98 and an efficiency of 77.8% at full load. Subsequently, the prototyped motor underwent comprehensive testing according to the IEC 60034-2-1:2014 standard methods for determining losses and efficiency. The efficiency of the SPIM, based on the measurement results obtained from testing in an accredited R&D laboratory compliant with ISO/EN 17025 standards, is calculated as 80.1%.

The successful realization of the SPIM design with enhanced efficiency not only aligns with the new regulations (EU)2019/1781 and (EU)2021/341 but also contributes to overall energy savings. By attaining high efficiency, SPIMs in the specified power range (0.12 kW ≤ PN ≤ 0wi.75 kW) can now meet the IE2 efficiency class requirements, enabling improved energy utilization in various industrial and household applications.

The findings contribute to the advancement of energy-efficient motor technology and have practical implications for reducing energy consumption and promoting sustainability in various industrial and household applications.

REFERENCES

[1] I. D. Chasiotis and Y. L. Karnavas, “On the design and manufacturing of small single phase induction motors toward super premium efficiency standards,” presented at the 2020 Int. Conf. on Electrical Machines (ICEM), Gothenburg, Sweden, pp. 2321-2327, 2020.

[2] Y. L. Karnavas, I. D. Chasiotis, “Design and manufacturing of a single-phase induction motor:A decision aid tool approach”, Int. Tran Electr Energ Syst. 27:e2357, 2017.

[3] D. Liang, V. Zhou, "Recent market and technical trends in copper rotor for high-efficiency induction motors", in Proc. of 2018 Int. Power Electronic Conf. (IPEC-Niigata 2018- ECCE Asia), Niigata, Japan, May 20-24, 2018.

[4] Udroiu, Nicoleta-Alina, and Carmen Georgeta Nicolae. "POSSIBILITIES TO REDUCE CO 2 EMISSIONS BY USING ELECTRIC MOTORS WITH HIGH ENERGY EFFICIENCY." Scientific Papers. Series D. Animal Science 65.1 (2022).

[5] T. Lubin, S. Mezani and A. Rezzoug, "Analytic Calculation of Eddy Currents in the Slots of Electrical Machines: Application to Cage Rotor Induction Motors," IEEE Transactions on Magnetics, vol. 47, no. 11, pp. 4650-4659, Nov. 2011.

[6] I. Chasiotis, Y. Karnavas, F. Scuiller, “Effect of rotor bars shape on the single-phase induction motors performance: An analysis toward their efficiency improvement”, Energies, 10.3390/en15030717, 15, 3, (717), 2022.

[7] Gui-Yu Zhou and Jian-Xin Shen, "Current harmonics in induction machine with closed-slot rotor," 2015 IEEE 2nd Int. Future Energy Electronics Conf. (IFEEC), Taipei, Taiwan, 2015.

[8] Lee KS, Ho Lee S, Park JH, Kim JM, Choi JY. “Experimental and analytical study of single-phase squirrel-cage induction motor consideringend-ring porosity rate,” IEEE Trans Magnet. 53(11) pp. 1-4. 2017.

[9] D. Sharma, R. K. Saini, and S. Pathania, “Design, analysis and selection of electric and magnetic loading for different rating of squirrel cage induction motors by using matlab gui software,” Int. J. Innovative Res. Elec. Electron. Instrum. Control Eng., vol. 3, no. 4, pp. 20-22, Apr. 2015.

[10] S.H. Choudhury, M.A. Uddin, N. Hasan, M. S. Alam, M. F. I. Bashar, “Impact of skin effect for the design of a squirrel cage induction motor on its starting performances”, International Journal of Engineering Science and Technology (IJEST), vol. 4, no.01 Jan. 2012. pp:362-366.

[11] C. Mademlis, I. Kioskeridis, and T.Theodoulidis, “Optimization of single-phase induction motors-Part I: Maximum energy efficiency control,” IEEE Trans. Energy Convers., vol. 20, no. 1, pp. 187–195, Mar. 2005.

[12] S. Shekhar, S. Kumar, S.K. Anand, S.K. Duve, P.D. Bharadwaj, “Design and programming for single phase induction motor”, International Journal of Engineering Science and Computing, April 2016.

[13] T.Z. Aung , E.E Cho, “Design calculation of single-phase permanent slip capacitor induction motor used in washing machine”, IRE Journals, vol. 3, no. 2, Aug 2019, pp:206-213.

[14] M. Farasat, A. M. Trzynadlowski, M. S. Fadali, “Efficiency improved sensorless control scheme for electric vehicle induction motors”, IET Electr. Syst. Transp., vol. 4, no. 4, pp. 122–131, 2014.

ACKNOWLEDGEMENT

We would like to thank Volt Elektrik Motor Company for providing laboratory facilities for the design, fabrication, and testing of the electric motor presented in this study.

BIOGRAPHIES

Serhat Aksun received the B.Sc. degree in electrical engineering from Kocaeli University in 2013. He received MSc. degree in Electrical&Electronics Engineering from Manisa Celal Bayar University in 2023. He works for the Volt Elektrik Motor Company as electrical design engineer.

Sezai Taskin received the B.Sc., M.Sc., and Ph.D. degrees from Marmara University, Istanbul, Türkiye, in 1999, 2001 and 2007, respectively. He worked as a Research Assistant at the Marmara University during his graduate studies. He joined the Electrical&Electronics Engineering Department at Manisa Celal Bayar University in 2012. His research interests include control system applications, solar PV systems, battery energy storage systems, and the smart operation of future power systems.

Ali Bakbak received the B.Sc. degree in electrical and electronics engineering from Niğde University, Niğde, Türkiye, in 2012, the M.Sc. degree in electrical and electronics engineering from Celal Bayar University, Manisa, Türkiye, in 2016, and the Ph.D. degree in electrical and electronics engineering from Ege University, Izmir, Türkiye, in 2021. He is currently a Faculty Member with Manisa Celal Bayar University, Manisa. His research interests include modeling, design, and control of electrical machines.